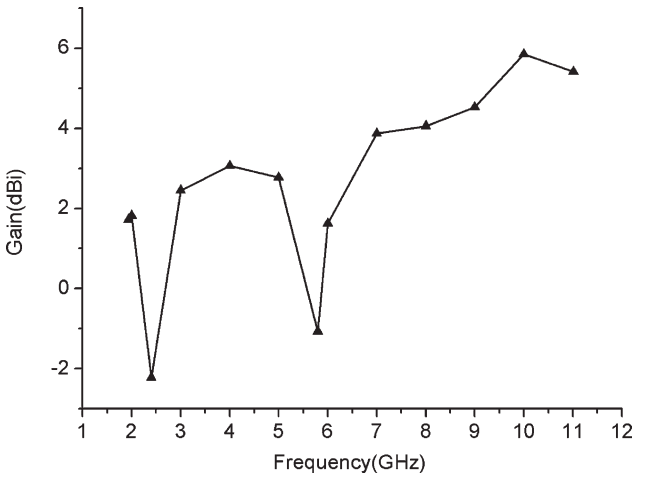

Figure 7 Measured gain of the proposed UWB antenna with dual band-notched function

gain decreases drastically at the notched frequency bands of 2.4 GHz and 5.8 GHz.

4. CONCLUSIONS

A compact UWB monopole antenna with dual band-notched characteristics for WLAN has been designed and manufactured. The dual band-notched characteristic at 2.4 GHz/5.8 GHz is achieved by cutting a folded stripline slot along the boundary of the radiation patch and by incorporating a pair of inverted-L-shaped slot on the ground. The proposed antenna has the frequency band from 2.2 GHz to 11 GHz for VSWR less than 2.0 with a rejection band in the frequency bands of 2.3–2.9 GHz and 5.5–6.3 GHz. The proposed antenna having dual frequency band-notched function and good electrical characters is promising for wireless communication applications.

REFERENCES

1. C.-H. Hsu, Planar multilateral disc monopole antenna for UWB application, Microwave Opt Technol Lett 49 (2007), 1101–1103.
2. S.H. Choi, H.C. Lee, and K.S. Kwak, Clover-shaped antenna for ultra-wideband communications, Microwave Opt Technol Lett 48 (2006), 2111–2113.
3. J.-C. Ding, Z.-L. Lin, Z.-N. Ying, and S.-L. He, A compact ultra-wideband slot antenna with multiple notch frequency bands, Microwave Opt Technol Lett 49 (2007), 3056–3060.
4. C.-H. Luo, C.-M. Lee, W.-S. Chen, C.-H. Tu, and Y.-Z. Juang, Dual band-notched ultra-wideband monopole antenna with an annular CPW-feeding structure, Microwave Opt Technol Lett 49 (2007), 2376–2379.
5. H.-J. Lee, Y.-H. Jang, J. Kim, and J.J. Yeo, Wideband circular slot antenna with tri-band rejection characteristics at 2.45/5.4/5.8 GHz, Microwave Opt Technol Lett 50 (2008), 1910–1914.
6. H.-J. Lee, Y.-H. Jang, J. Kim, and J. Choi, Wideband monopole antenna with (2.4 GHz/5 GHz) dual band-stop function, Microwave Opt Technol Lett 50 (2008), 1646–1649.
7. S.-H. Lee, J.-W. Baik, and Y.-S. Kim, A coplanar waveguide fed monopole ultra-wideband antenna having band-notched frequency function by two folded-stripline, Microwave Opt Technol Lett 49 (2007), 2747–2750.

SIZE-REDUCED DEFECTED GROUND MICROSTRIP DIRECTIONAL COUPLER

Ashraf S. Mohra,[1] Majeed A. Alkanhal,[1] and Esmat A. Abdullah[2]
[1] Electrical Engineering Department, King Saud University, College of Engineering, Saudi Arabia; Corresponding author: amohra@ksu.edu.sa
[2] Electronics Research Institute, Egypt

Received 20 November 2009

ABSTRACT: *In this article, size reduction and harmonic suppression in coupled-lines microstrip directional couplers is attained using dumbbell, and reshaped dumbbell slots, as defected patterns, specifically placed under the metering position in the ground plane. Quantitative investigation of the performance of the directional coupler as controlled by the variations of the DGS rectangular slots height, DGS gap length, and the DGS reshaped rectangular slot height is presented. This concept is further illustrated experimentally for a 12 dB coupler realized on RT/Duroid 5880 substrate. The proposed DGS design confers size reduction because of the shift of the operating frequency to lower values. The measurements are in a good agreement with the simulated results and emphasize the size reduction and the harmonics suppression of the DGS coupled-lines microstrip directional coupler.* © 2010 Wiley Periodicals, Inc. Microwave Opt Technol Lett 52: 1933–1937, 2010; Published online in Wiley InterScience (www.interscience.wiley.com). DOI 10.1002/mop.25410

Key words: *microstrip directional coupler; dumbbell slots; metering slots; defected ground structure*

1. INTRODUCTION

Directional couplers with parallel microstrip coupled transmission lines are widely utilized for various radio frequencies (RF) and microwave applications, because they can be easily implemented with other devices and circuits. They have been applied for microwave components such as dividers, combiners, attenuators, phase shifters, balanced and double-balanced mixers, and balanced amplifiers used in microwave systems such as beam forming network and feed networks in antenna arrays, vector network analyzers, spectrum analyzers, radar receivers, and power level sensors. They have several advantages, such as

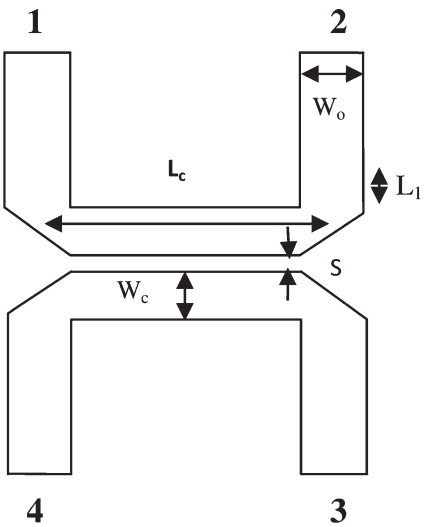

Figure 1 Conventional microstrip directional coupler

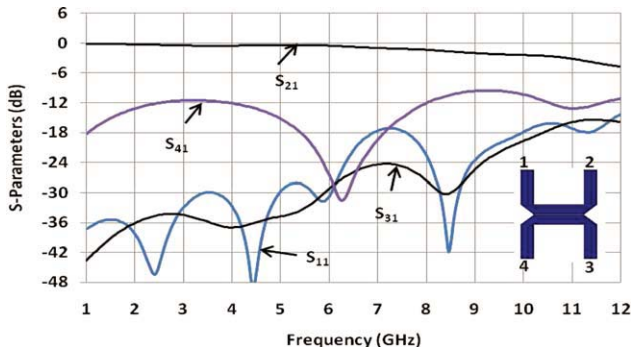

Figure 2 The simulated S-parameters for the conventional microstrip directional coupler. [Color figure can be viewed in the online issue, which is available at www.interscience.wiley.com]

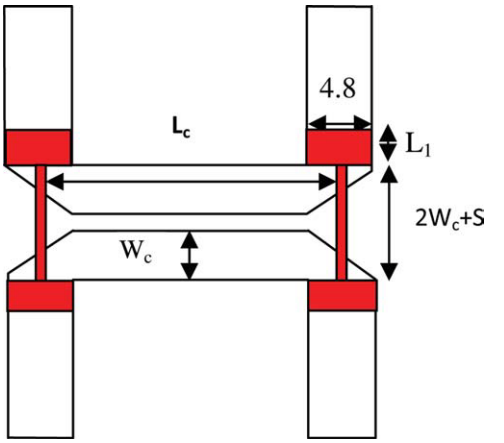

Figure 3 The DGS directional coupler showing the rectangular slots height (L_1). [Color figure can be viewed in the online issue, which is available at www.interscience.wiley.com]

manufacturability, repeatability, and low-cost. The first directional coupler was reported in 1922 [1], and significant improvements were made later [2, 3]. Numerous articles [4–9] explained the theory and applications of the parallel coupled transmission lines that have equal impedance terminations.

Microstrip directional couplers generally require quarter-wave transmission lines measured at the design center frequency, which leads to impractical dimensions in lower microwave range applications like RFID system and the WiFi/WiMAX RF applications that require lightweight, cost effective and small size components. Conventionally, several methods to reduce the size of individual transmission lines have been proposed by researchers. Size reduction can be achieved by using the folded line configurations [10]. The resultant circuit area using such a method would be still large. Another method is accomplished by adopting lumped element components, which is suitable in MMIC application [11–14].

In this article, size reduction of microstrip coupled lines using defected ground with dumbbell slots is used to yield size-reduction for microstrip directional couplers. The defected ground structures (DGS) are particularly added beneath the matching points (metering positions) between the microstrip coupled lines and the terminating transmission lines. Typically a defected ground microstrip circuit is attained by etching in the backside metallic ground plane [15–21]. These defections in the ground layer disturb the current distribution in the ground plane and increase the effective inductance and capacitance of the microstrip line. The microstrip line with DGS pattern provides bandgap effect at certain frequencies [18–21]. Therefore, the DGS is usually modeled by LC resonance circuit using circuit analysis methods.

In the following sections, the analysis for the effect of the proposed DGS on the performance of the microstrip directional coupler is presented. The effect of the rectangular dumbbell slot heights, the slot separations, and the reshaped rectangular slot height on the operating band shift for the microstrip directional coupler is quantitatively investigated. These analysis are carried out for a microstrip coupler with (−12 dB) coupling, design, and realized on RT/Duroid 5880 ($\varepsilon_r = 2.2$, $h = 1.5748$ mm) at 3 GHz operating frequency. As an example, one of the designed DGS microstrip directional coupler has been realized, and then its performance represented by the S-parameters were measured and reported. The reduction in size and the harmonic suppression accomplished in the proposed DGS coupled line coupler structure are described.

2. EFFECT OF THE COUPLED-LINES WITH DGS PATTERN ON THE FREQUENCY SHIFT

First a microstrip directional coupler with (−12 dB) coupling coefficient was designed on RT/Duroid 5880 ($\varepsilon_r = 2.2$, $h = 1.5748$ mm) to operate at 3 GHz. The dimensions of this coupler shown in Figure 1 are as follows: $W_c = 4.25$ mm, $S = 0.3$ mm, $L_c = 18.5$ mm, and $W_o = 4.8$ mm (corresponding to 50 Ω terminating port). This coupler was simulated using IE3D software package and the results are shown in Figure 2. The coupler performance at the operating frequency can be deduced as coupling (S_{41}) equal to (−12 dB) where the reflection (S_{11}) and isolation (S_{31}) are less than −30 db. The next harmonic for this coupler is appeared to be close to 9 GHz.

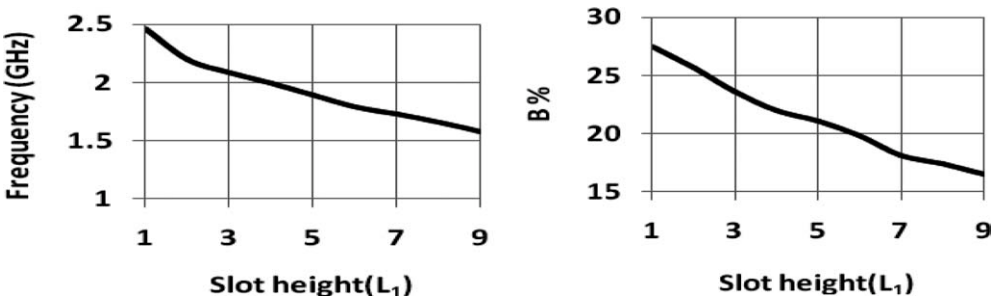

Figure 4 The frequency and bandwidth ratio (B) against the slot height (L_1)

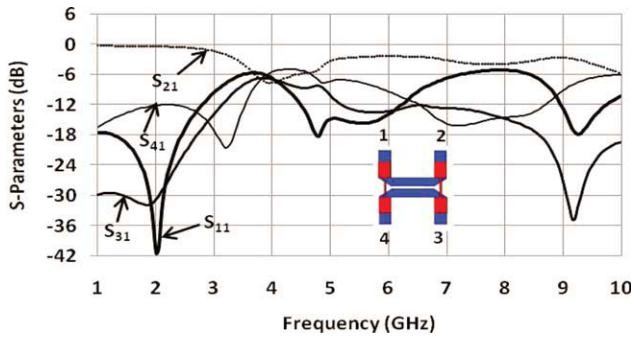

Figure 5 The simulated S-parameters for DGS microstrip directional coupler when $L_1 = 4.0$ mm. [Color figure can be viewed in the online issue, which is available at www.interscience.wiley.com]

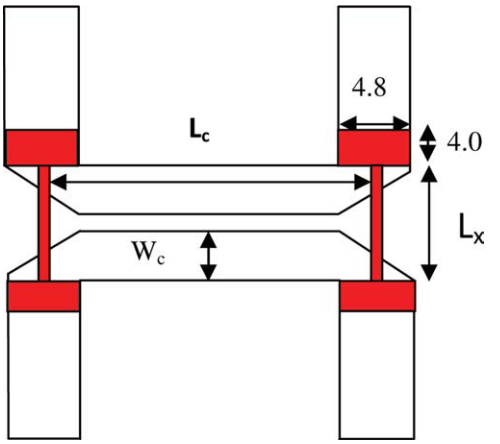

Figure 6 The DGS directional coupler showing the slots separation (L_x). [Color figure can be viewed in the online issue, which is available at www.interscience.wiley.com]

Next, the effect of the DGS pattern location and dimensions on the performance of the microstrip directional coupler will be discussed. The effect of the DGS rectangular slot height, DGS gap length, and DGS reshaped rectangular slot height on the coupler performance will be outlined in the following subsections.

2.1. DGS Rectangular Slot Heights Variations

By adding defected ground dumbbell slots under the parallel coupled lines in the metering position of the above coupler as shown in Figure 3, the performance of the coupler will be affected and shifted to a lower frequency band. Carrying out the design numerical simulations using different rectangular slot heights (L_1), it is observed that as the slot height (L_1) increases, both of the resonance frequency and the bandwidth ratio (B) for the DGS coupler decrease as represented in Figure 4. The resonance frequency and the bandwidth ratio are calculated within the ranges ($S_{21} = -12 \pm 0.5$ dB and S_{11}, $S_{31} < -18$ dB). The resonance frequency of the DGS microstrip directional coupler (1.5–2.5 GHz) is noticeably lower than that of the same size conventional coupler (3 GHz). This indicates a remarkable size reduction opportunity for the 12 db coupler.

Figure 5 depicts the performance of a same size directional coupler with DGS dumbbell slots of dimension (4.8 mm $\times$ 4.0 mm) and $L_1 = 4.0$ mm. The DGS coupler shows even a better performance with coupling coefficient (S_{41}) around -12 dB at 2.05 GHz and with reflection and isolation coefficients (S_{11} and S_{31}) less than -28 dB. The resonance frequency and the bandwidth ratio (within $S_{21} = -12 \pm 1.0$ dB and S_{11}, $S_{31} < -20$ dB) are 2.1 GHz and 47%, respectively. Besides the size reduction that can be accomplished using this DGS coupler, it also has a remarkable harmonic suppression near the 9 GHz band.

2.2. DGS Gap Length Variations

The effect of the gap-length (L_x) on the frequency performance of the above DGS directional coupler is investigated in this section. The dumbbell slot dimensions are held constant (4.8 mm $\times$ 4 mm), whereas the gap length (L_x) is varied as shown in Figure 6. Figure 7 depicts the results of this investigation. As the length of the gap between the upper and lower slots (L_x) increases, the resonance frequency and the bandwidth ratio (B) of the directional coupler decrease. The resonance frequency and the bandwidth ratio calculations were measured within the range of ($S_{21} = -12 \pm 0.5$ dB and S_{11}, $S_{31} < -18$ dB). This type of DGS microstrip coupler also achieves a good size reduction.

The simulation results for DGS microstrip directional coupler with slot dimensions (4.0 mm $\times$ 4.8 mm), $L_x = 8.8$ mm, are shown in Figure 8. It is clear that, the operating frequency of the DGS coupler has moved to 2.1 GHz instead of 3 GHz, which enables a good size reduction. The coupling coefficient (S_{41}) is nearly (-12 dB) at 2.1 GHz, whereas the reflection and isolation coefficients (S_{11} and S_{31}) are less than (-28 dB). The simulated directional coupler has harmonic suppression up to 10 GHz.

2.3. DGS Metering Reshaped Slot Height Variations

In this case, the defected ground slot is reshaped and brought to be precisely under the matching position (metering section) between the coupled transmission line and the terminating (50 Ω) lines as shown in Figure 9. The effect of varying the length L_2 on the resonance frequency and the bandwidth ratio

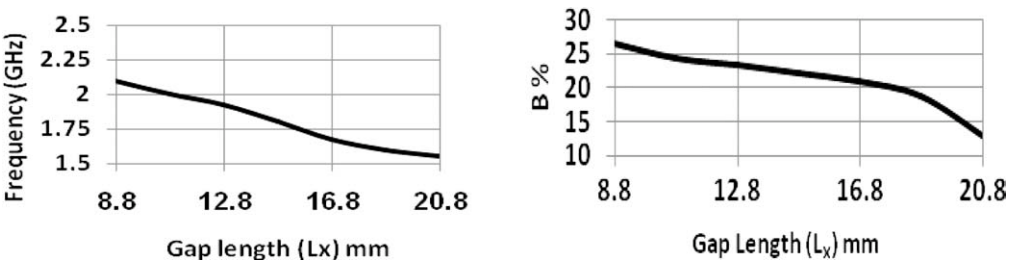

Figure 7 The frequency and bandwidth ratio (B) against the gap length (L_X)

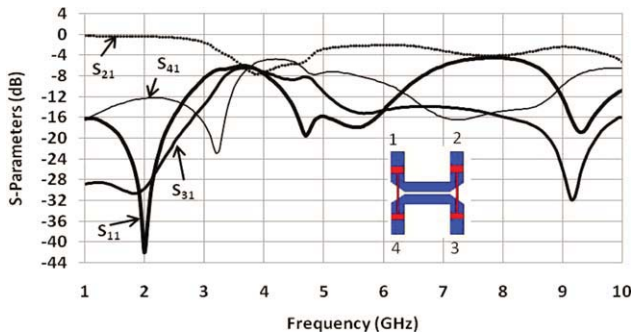

Figure 8 The simulated S-parameters for DGS microstrip directional coupler when $L_x = 8.8$ mm. [Color figure can be viewed in the online issue, which is available at www.interscience.wiley.com]

(B) is shown in Figure 10. The resonance frequency and the bandwidth ratio calculations were considered within the condition ($S_{21} = -12 \pm 1.0$ dB and S_{11}, $S_{31} < -20$ dB). This case also, achieves a good size reduction for the microstrip directional coupler.

The simulation results for the reshaped DGS microstrip directional coupler with $L_2 = 3$ mm, are shown in Figure 11. The operating frequency of the reshaped DGS coupler has moved to 2.25 GHz instead of 3 GHz, which enables a good size reduction. The coupling coefficient (S_{41}) is nearly (-12 dB) at 2.25 GHz, whereas the reflection and isolation coefficients (S_{11} and S_{31}) are less than (-30 dB). The reshaped DGS coupler has harmonic suppression up to 10 GHz.

From the previous discussion, it can be concluded that size reduction and harmonic suppression can be obtained using dumbbell and reshaped dumbbell slots as defected patterns under the metering position in the ground plane of a conventional microstrip coupled-lines directional coupler. The performance of the coupled lines and hence of the directional coupler is greatly controlled by the variations of the rectangular DGS slots height, DGS gap length, and DGS reshaped slot height. The resonance frequency is moved to lower values, which achieves a noticeable size reduction. For all investigated DGS scenarios, the microstrip directional coupler with DGS achieves improved harmonics suppression too.

3. FABRICATION AND MEASUREMENTS

To illustrate the above concept and investigations of the effect of the DGS on the microstrip directional coupler performance, the configuration shown in Figure 9 was selected for further experimental investigations. This (12 dB) coupler was realized on RT/Duroid 5880 ($\varepsilon_r = 2.2$, $h = 1.5748$ mm). The dimensions are $W_c = 4.25$ mm, $S = 0.3$ mm, $L_c = 18.5$ mm, $W_o = 4.8$ mm, and $L_2 = 3$ mm, which are chosen as for the covenantal coupler operating at 3 GHz. The measured S-parameter for this reshaped DGS coupler is shown in Figure 12. Within the range of ($S_{21} = -12 \pm 1.0$ dB and S_{11}, $S_{31} < -20$ dB), the resonance frequency is shifted to 2.102 GHz, which enables the desired size reductions, and the bandwidth ratio is 24.6%. The DGS microstrip coupler achieves more than 30% size reduction and, at the same time, attains a good harmonics-suppression up to beyond 10 GHz.

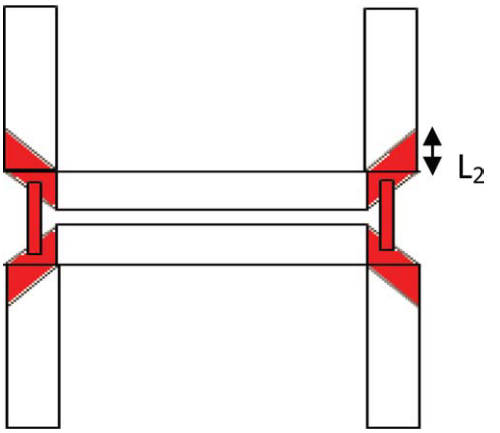

Figure 9 The DGS directional coupler showing the reshaped rectangular slots height (L_2). [Color figure can be viewed in the online issue, which is available at www.interscience.wiley.com]

4. CONCLUSIONS

In this article, size reduction and harmonic suppression in microstrip coupled-lines directional couplers is attained using dumbbell and reshaped dumbbell slots as defected patterns, specifically, placed under the metering position in the ground plane. The performance and the operating frequency of the coupled lines and hence of the directional coupler is greatly controlled by the variations of the DGS slots height, DGS gap length and DGS reshaped slot height. This concept is illustrated by simulation and experimental measurements of a realized (12 dB) coupler on RT/Duroid 5880 ($\varepsilon_r = 2.2$, $h = 1.5748$ mm). The realized DGS microstrip directional coupler achieves a size reduction, so the DGS coupler is less than 70% of the conventional coupler. In addition, the defected ground coupler accomplishes a good harmonic suppression.

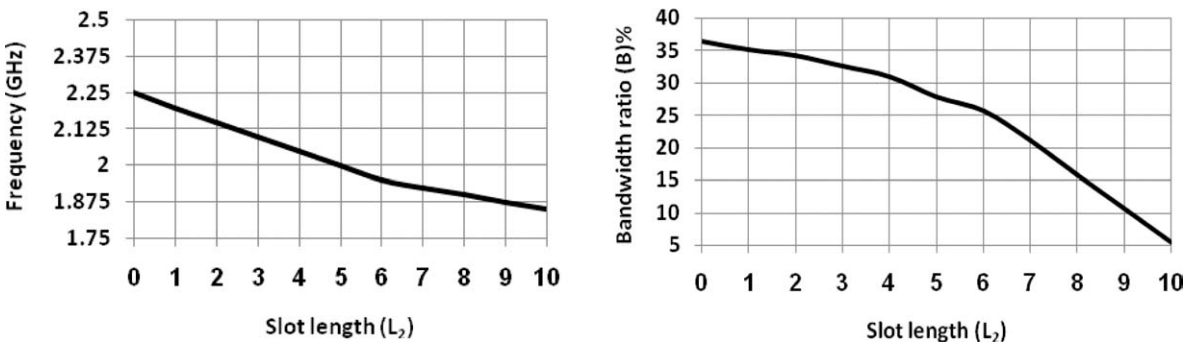

Figure 10 The frequency and bandwidth ratio (B) against the reshaped rectangular slot height (L_2)

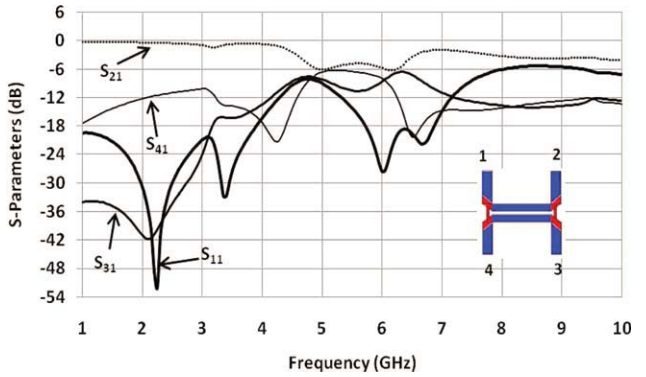

Figure 11 The simulated S-parameters for the DGS microstrip directional coupler when $L_2 = 3.0$ mm. [Color figure can be viewed in the online issue, which is available at www.interscience.wiley.com]

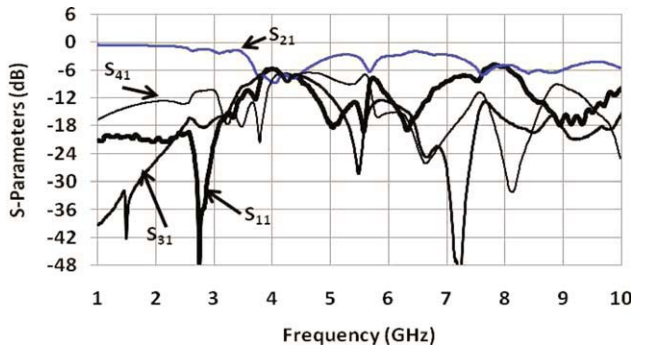

Figure 12 The Measured S-parameters for the DGS microstrip directional coupler when $L_2 = 3.0$ mm. [Color figure can be viewed in the online issue, which is available at www.interscience.wiley.com]

ACKNOWLEDGMENTS

The authors would like to acknowledge the assistance and the financial support for this work that provided by the Research Center, College of Engineering at King Saud University.

REFERENCES

1. S.B. Cohn and R. Levy, History of microwave passive components with particular attention to directional couplers, IEEE Trans Microwave Theory Tech 32 (1984), 1046–1054.
2. E.M.T. Hones and J.T. Bolljahn, Coupled-strip-transmission-line filters and directional couplers, IRE Trans Microwave Theory Tech 4 (1956), 75–81.
3. S.B. Cohn, Parallel-coupled transmission line resonators, IRE Trans Microwave Theory Tech 6 (1958), 223–231.
4. G.L. Matthaei, Interdigital bandpass filters, IRE Trans Microwave Theory Tech 10 (1962), 479–491.
5. R. Levy, General synthesis of asymmetric multi-element coupled transmission line directional couplers, IEEE Trans Microwave Theory Tech 11 (1963), 227–231.
6. G.I. Zysman and A.K. Johnson, Coupled transmission line networks in an inhomogeneous dielectric medium, IEEE Trans Microwave Theory Tech 17 (1969), 753–759.
7. E.G. Cristal, Coupled-transmission-Line directional couplers with coupled lines of unequal characteristic impedances, IEEE Trans Microwave Theory Tech 14 (1966), 337–346.
8. J.P. Shelton, Impedances of offset parallel-coupled strip transmission lines, IEEE Trans Microwave Theory Tech 14 (1966), 7–15.
9. J.P. Shelton and J.A. Mosko, Synthesis and design of wideband equal ripple TEM directional couplers and fixed phase shifters, IEEE Trans Microwave Theory Tech 14 (1966), 462–473.
10. M.J. Park and B. Lee Compact foldable coupled-line cascade couplers, IEE Proc Microwave Antennas Propag 153 (2006), 237–240.
11. L.G. Maloratsky, Passive RF & Microwave Integrated Circuits, Newnes, 2004, pp. 117–162.
12. M. Caulton, B. Hershenov, S.P. Knight, and R.E. Debrecht, Status of lumped elements in microwave integrated circuit-present and future, IEEE Trans Microwave Theory Tech 19 (1971), 588–599.
13. J. Post, An exact lumped-element equivalent circuit model for transmission-line transformers formed from coupled microstrip lines, Microwave Opt technol lett 49 (2007), 2984–2988.
14. T.N. Kuo, Y.S. Lin, C.H. Wang, and C.H. Chen, A compact LTCC branch-line coupler using modified-T equivalent-circuit model for transmission line, IEEE Microwave Wireless Compon Lett 16 (2006), 90–92.
15. C.-S. Kim, J.-S. Park, D. Ahn, and J.-B. Lim, A Novel 1-D Periodic Defected Ground Structure for Planar Circuits, IEEE Microwave Guid Wave Lett 10 (2000), 131–133.
16. D. Ahn, J.S. Park, C.S. Kim, J. Kim, Y. Qian, and T. Itoh, A design of the low pass filter using novel microstrip defected ground structures, IEEE Trans Microwave Theory Tech 49 (2001), 86–92.
17. H.-W. Liu, Z.-F. Li, X.-W. Sun, and J.-F. Mao, An Improved 1-D Periodic Defected Ground Structure for Microstrip Line, IEEE Microwave Wireless compon Lett 14 (2004), 180–182.
18. J.-S. Hong and B.M Karyamapudi, A General Circuit Model for Defected Ground Structures in Planar Transmission Lines, IEEE Microwave Wireless compon Lett 15 (2005), 706–708.
19. S.K. Parui and S. Das, Simple Defected Ground Structure with Elliptical Lowpass filtering Response, Proceedings of Asia-Pacific Microwave Conference, Bangkok, Thailand, 2007.
20. J. Yang and W. Wu, Compact Elliptic-Function Low-Pass Filter Using Defected Ground Structure, IEEE Microwave Wireless compon Lett 18 (2008), 578–580.
21. A.S. Mohra, Compact Lowpass Filter with Sharp Transition Band Based on Defected Ground Structures, Prog Electromagnetics Res Lett 8 (2009), 83–92.

EXPERIMENTAL OBSERVATION OF PHOTO-EXCITED ELECTRON DEPLETION FOR STABILITY IMPROVEMENT IN A LITHIUM NIOBATE POLARIZATION CONVERTER

Ruey-Ching Twu,[1] Hsuan-Hsien Lee,[2] and Hao-Yang Hong[1]
[1] Department of Electro-Optical Engineering, Southern Taiwan University, Tainan 710, Taiwan; Corresponding author: rctwu@mail.stut.edu.tw
[2] Department of Electrical Engineering, Southern Taiwan University, Tainan 710, Taiwan

Received 26 November 2009

ABSTRACT: *The relations between conversion stabilities and photo-excited electron-depletion effects have been experimentally evaluated in a Zn-indiffused lithium niobate polarization converter, for the first time. A simple method with a biased voltage and laser trimming was performed to observe these phenomena. The results show that the stable conversions for both polarities of applied polarization-conversion voltages are achievable due to the depletion of photo-excited electrons in the waveguides.* © 2010 Wiley Periodicals, Inc. Microwave Opt Technol Lett 52: 1937–1941, 2010; Published online in Wiley InterScience (www.interscience.wiley.com). DOI 10.1002/mop.25384

Key words: *polarization converter; lithium niobate; photorefractive*